ELSEVIER

Ultramicroscopy 79 (1999) 265–271

ultramicroscopy

www.elsevier.nl/locate/ultramic

Performance of a microsphere plate electron multiplier in APFIM applications

S.J. Sijbrandij, M.K. Miller*

Metals and Ceramics Division, Oak Ridge National Laboratory, Building 5500, MS 6376, P.O. Box 2008, Oak Ridge, TN 37831-6376, USA

Received 12 September 1998; received in revised form 27 December 1998

Abstract

The microsphere plate (MSP) is a recently introduced electron multiplier, that is comparable in principle of operation to the well-known microchannel plate. The performance of a MSP detector has been evaluated for field ion imaging and single atom detection in time-of-flight atom probe mass spectrometry. The image performance of a MSP is not sufficient for obtaining high-quality field ion images, due to the lack of spatial resolution as well as the granularity observed in the images. Gain, pulse height resolution, and temporal resolution obtained from one double thickness MSP are sufficient for use in a time-of-flight single atom sensitivity detector. The detection efficiency was estimated to be $\sim 42\%$ for ions in the energy range between 10 and 40 keV. The operation of the MSP detector was successfully demonstrated in a typical atom probe application. Published by Elsevier Science B.V.

Keywords: Election multiplier; Microsphere plate; Detector

1. Introduction

Electron multipliers are commonly used in atom probe field ion microscopes [1]. Microchannel plates (MCPs) [2] are normally used as image intensifiers for the field ion image, and microchannel plate stacks, and to a lesser extent dynode stacks or channeltrons [3] are used in the single atom detector of the atom probe mass spectrometer. Recently, a new type of electron multiplier, the microsphere plate (MSP), has been commercially introduced.[1] The MSP is a sintered plate of ~ 50 μm-diameter glass beads. The electron multiplication process takes place in the interstices between these beads when a voltage is applied between the front and rear surfaces, which are covered with thin layers of nichrome, as shown in Fig. 1.

Despite the similarity in operating principle there are some significant differences between MCPs and MSPs. Advantages of MSPs are higher gain and less stringent vacuum requirements. The absence of long electron travel paths inside MSPs minimizes ionic feedback, which allows biases of up to 3.5 kV to be used at pressures exceeding 1 Pa [4]. A disadvantage of MSPs is lower spatial resolution, typically 2.0–2.5 line-pairs/mm, due to the spreading out of the electron avalanche within the MSP, and also due to the randomness of the sphere stacking within the plate, as well as the

* Corresponding author. Tel.: + 1-423-574-4719; fax.: + 1-423-574-0641.

E-mail address: millermk@ornl.gov (M.K. Miller)

[1] El-Mul Technologies Ltd., P.O. Box 571, Yavne 81104, Israel; Internet: http://www.el-mul.co.il.

0304-3991/99/$ - see front matter Published by Elsevier Science B.V.
PII: S0304-3991(99)00065-0

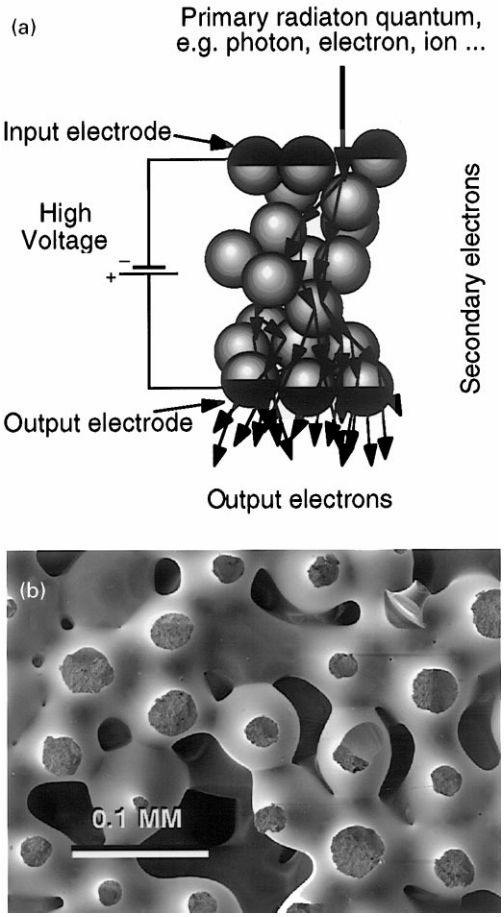

Fig. 1. (a) Schematic diagram illustrating the architecture and operation of a MSP electron multiplier, (b) Scanning electron microscope image of a MSP.

larger "unit size" (50 μm diameter beads in MSPs compared to 8–25 μm channel spacing in MCPs). Another disadvantage is the lower geometrical open area ratio (OAR), 20–40%, which compares to typically 50–70% for MCPs. However, the effective OAR may be significantly higher in MSPs, since most of the input surface may be active due to a strong funneling effect. This effect is also known in MCPs ([5] and references therein).

MSPs are less expensive than similarly sized MCPs, and are said to be less fragile than MCPs. MSPs are currently available in single thickness, 0.7 mm, and double thickness, 1.4 mm plates in a range of diameters between 12 and 70 mm. The simple manufacturing process may allow the fabrication of larger and custom-shaped plates.

The performance of MSPs for the detection of UV radiation has been described elsewhere [6–11]. This paper presents the performance of these plates in field ion microscopy and atom probe applications.

2. Experimental

A double thickness (1.4 mm), 33-mm-diameter MSP was used in the test detector. A proximity focused (P-20) phosphor screen on a fiberoptic substrate was located 2 mm from the MSP output. This screen was used to collect the electrons generated in the multiplication process and enabled the distribution of the electrons to be visually observed. A square nickel mesh with 98% transparency and a wire spacing of 5 mm was positioned at a distance of 5 mm in front of the MSP input. For some experiments the mesh was replaced by a nickel test-mask or aperture plate. The active portion of the detector was 25 mm in diameter.

The MSP input was biased -50 V with respect to the grounded vacuum chamber, in order to repel secondary electrons generated from ion impacts on the vacuum chamber walls. The MSP output was biased up to $+3.5$ kV with respect to the input. Biases in the 2.0–2.5 kV range were typically used during field ion microscopy, and in the 2.5–3.5 kV range for the detection of single ions. The voltage across the gap between the MSP output and phosphor screen was set as a fixed ratio (120%) of the MSP bias. The mesh could be biased up to ± 2.0 kV with respect to the MSP input, for the purpose of studying the "funneling effect" at the MSP input. A 100 pF high-voltage capacitor was used to couple the signal pulses from the phosphor screen to the timing and counting electronics. No amplification was used between the MSP detector and subsequent electronics. Pulse height distributions were derived from measurements of detection count rate versus threshold (with the use of a LeCroy 4608 discriminator) following a method described in Ref. [12].

For comparison, field ion images were also recorded on a standard MCP and phosphor screen

combination. This detector had a Philips double thickness MCP with a 12.5 μm pore diameter, an active area 62 mm in diameter, and was positioned at ~75 mm from the specimen.

The MSP detector was mounted on an auxiliary port of a custom built atom probe at ~275 mm from the specimen. For comparison, atom probe experiments were also performed on the ORNL energy compensated atom probe [13], equipped with a Galileo 3025 Chevron MCP detector. The base pressures of both atom probes were $<10^{-8}$ Pa. All atom probe analyses were performed with a specimen temperature of 70 K, pulse fractions of 15–20%, and a pulse frequency of 1500 Hz generated with a solid state pulser. A LeCroy 4208 time-to-digital converter, with 1 ns resolution, was used for the time-of-flight measurements.

Ion energies were in the range of 10–20 keV for the field ion microscopy experiments, and 20–40 keV for the atom probe experiments.

3. Results

Field ion micrographs of a tungsten specimen recorded on the MCP and MSP detectors are shown in Fig. 2. The MSP images exhibit significant variations in output intensity or granularity on the scale of a few 100 μm. This granularity is caused by the random structure of the MSP plates, with the scale of the variations corresponding to a few sphere diameters. Therefore, the image performance of the MSP is not sufficient for obtaining high-quality field ion images, as expected. However, it is also clear that when used in a single atom probe detector, that the imaging performance should be adequate to allow alignment and focusing of the ion beam in a conventional atom probe, or to correlate the selected area of analysis with the full field ion image in a three-dimensional atom probe.

The pulse height distributions (PHDs) with the mesh operated at biases of −50 V and +50 V with respect to the MSP input, with a MSP bias of 3.0 kV is shown in Fig. 3. The PHD of the dark noise is also shown for this bias (noise PHDs were found to be independent of mesh bias, as expected). The PHDs exhibit a well-defined peak shape with

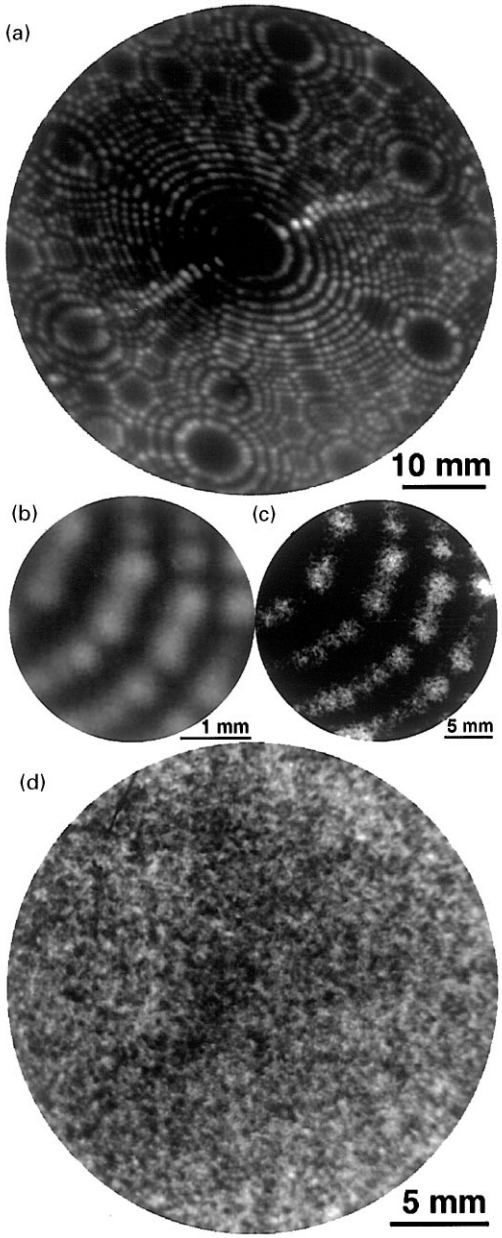

Fig. 2. Field ion micrographs from a tungsten specimen, at a temperature of ~70 K, obtained with 2×10^{-3} Pa neon image gas. (a) MCP image, with the specimen at best image voltage (12.0 kV). (b) Enlargement of (a). (c) MSP image of the same area as shown in (b). (d) MSP image, with the specimen just below field evaporation voltage (19.5 kV), producing uniform irradiation. Line-damage near "11 o'clock" is due to a scratch on the phosphor screen. Scale markers indicate the actual sizes of the images on the detectors.

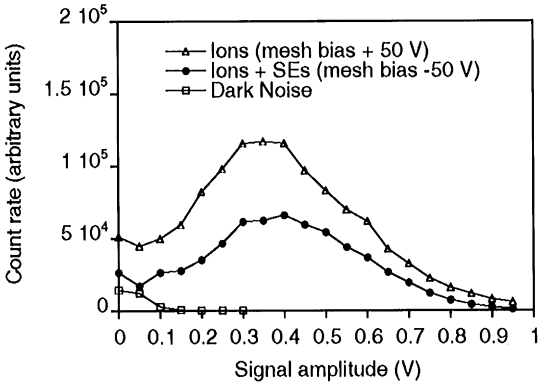

Fig. 3. Pulse height distributions obtained with mesh biases of −50 and +50 V with respect to the MSP input. 19.1 keV Ne^{1+} ions (at a rate of ~2000 counts per second, uniformly distributed over the MSP input surface) were used as the primary irradiation. The MSP bias was 3.0 kV. The PHD for the dark noise at this setting is also shown.

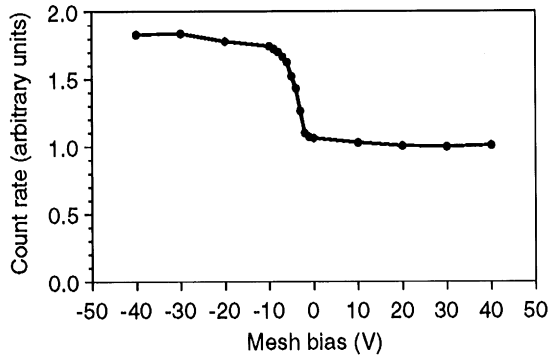

Fig. 4. The detection count rate from a stable 19.1 keV Ne^{+} ion source as a function of mesh bias with respect to MSP input, obtained with a 150 mV threshold applied. A rate of ~2000 counts per second uniformly distributed over the MSP input was used. The MSP bias was 3.0 kV.

resolutions of the order of 100% full-width at half-maximum (FWHM). The dark noise level in MSPs appeared to be higher than that of MCP detectors, especially at high bias, but the noise amplitude drops off rapidly, and can be removed by applying a small threshold voltage (e.g. 100 mV), without losing a significant proportion of the signal. Note that the modal pulse height of the unamplified signal is ~400 mV, which is substantially higher than that typically obtained with a double MCP detector. This large signal amplitude removes the need for amplification between detector and timing electronics. It is concluded that the gain and pulse height resolution obtainable from a single double-thickness MSP are sufficient for use in a single atom detector in an atom probe application.

The count rate was found to be significantly higher with the mesh biased negatively. This is directly demonstrated in the variations of detection rate of a stable ion source as a function of the mesh bias shown in Fig. 4. A factor of 1.8 improvement in detection rate is obtained when the mesh bias is switched from +50 V to −50 V, with most of this improvement taking place in the range between 0 V and −10 V. This confirms the existence of strong funneling effects at the MSP input. The +50 V and −50 V mesh biases correspond to the situations in which most of the secondary electrons resulting from ion impacts on the nominally dead area on the input surface are removed from the input, and returned to the input, respectively. The shapes of the PHDs do not show large differences, which suggests that the PHDs for the primary ion impacts and secondary electron impacts are similar. However, relatively high count rates were observed at large pulse heights at a mesh bias of −50 V. This is probably due to single ion impacts causing the emission of multiple secondary electrons, each of which trigger a separate electron multiplication process at different locations on the input surface.

A time spectrum obtained from a monoisotopic cobalt specimen is shown in Fig. 5. This spectrum was accumulated in a pressure of 3×10^{-4} Pa of neon so that the field ion image was clearly visible on the MSP detector during analysis. The randomly distributed background noise in the spectrum is mainly due to the high background pressure. No afterpulsing of the detector was observed at this high background pressure. It should be noted that the spread in flight times ($dt/t \sim 1/230$ FWHM or $dm/m \sim 1/115$) is mainly caused by the spread in effective acceleration voltage of the field evaporated ions due to the slow rise time of the pulser (−2.5 ns) and the lack of energy compensation. Tremsin et al. [6] have modeled the microsphere plate and calculated transit times in the order of 250–400 ps at

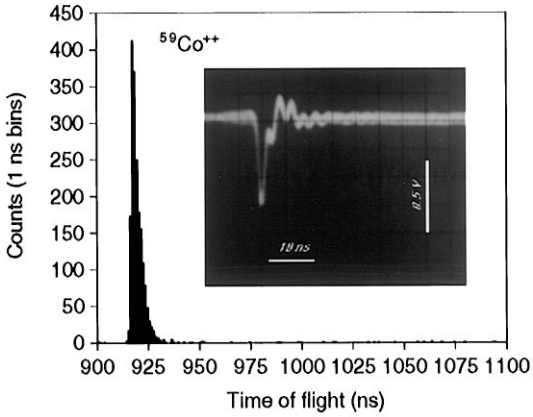

Fig. 5. Time spectrum from a cobalt specimen, obtained in a background of 3×10^{-4} Pa neon. The MSP bias was 3.0 kV. Specimen voltage: 13.5 kV, pulse fraction: 20%, specimen temperature: 70 K. Inset shows the oscillogram of a single (unamplified) detection event. The risetime of ~ 1 ns is limited by the oscilloscope and by the impedance mismatching in the electronics. The ringing in the tail of the pulse is probably due to the impedance mismatch, rather than being a characteristic of the MSP.

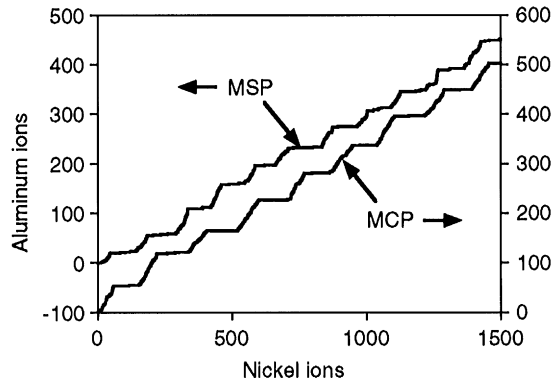

Fig. 6. Ladder diagram of atom probe analyses of an $L1_2$-ordered Ni_3Al specimen along a 100 pole on an MSP detector and a Chevron MCP detector. The MSP bias was 3.0 kV, and the mesh bias was -50 V with respect to the MSP input. Specimen voltage: 17 kV, pulse fraction: 15%, specimen temperature: 70 K.

biases between 2.6–4 kV with transit time spreads in the order of 50 ps FWHM, which is an order of magnitude smaller than the resolution of the timers typically used for the flight time measurements. It is therefore concluded that the temporal resolution obtainable from an MSP should be sufficient for use in an atom probe mass spectrometer.

In order to test the detection efficiency, an $L1_2$-ordered Ni_3Al specimen was analyzed along a (1 0 0) ordered pole. The same specimen was analyzed on an atom probe equipped with the MSP detector, and on one equipped with a double-MCP detector, under similar conditions, with negligible evaporation between the two experiments. The ladder diagrams from both analyses, shown in Fig. 6, clearly indicate the alternating pure nickel and mixed nickel + aluminum planes. On average 92 ± 3 ions were collected per atomic plane with the MSP detector, and 113 ± 3 ions were collected with the MCP detector. However, some minor differences between the two instruments have to be taken into account. The acceptance angle on the MSP detector was 10% larger than that on the MCP detector, leading to a 21% larger effective area of analysis for the MSP detector. Previous calibration experiments on the MCP detector have established that it has a detection efficiency of 62 ± 2%. From these parameters, the number of ions per atomic plane available for detection on the MSP detector was estimated to be 220 ± 10. Therefore, the detection efficiency of the MSP was estimated to be 42 ± 3%. It should be noted that the MSP detection efficiency was optimized by biasing a mesh in front of the input, but that the MCP detector was not operated in optimized condition. Improvements by a factor of 1.25 [5]–1.4 [14] may be achieved for MCP detectors by the incorporation of a biased mesh, which can increase the detection efficiency of an MCP detector to between 75 and >85%. The larger improvement observed for the MSP detector (factor 1.8, Fig. 4) is consistent with its smaller open area ratio. Although the MSP detector was successfully operated in a typical atom probe application, these experiments suggest that the detection efficiency of the MSP detector is significantly lower (by a factor of up to ~ 2) than that of an MCP detector when used for the detection of 10–40 keV ions. However, it is not an order of magnitude smaller than that of MCPs, as was reported for the detection of UV radiation [9].

The spatial resolution from the position determination of single atom impacts has also been characterized in order to evaluate the performance

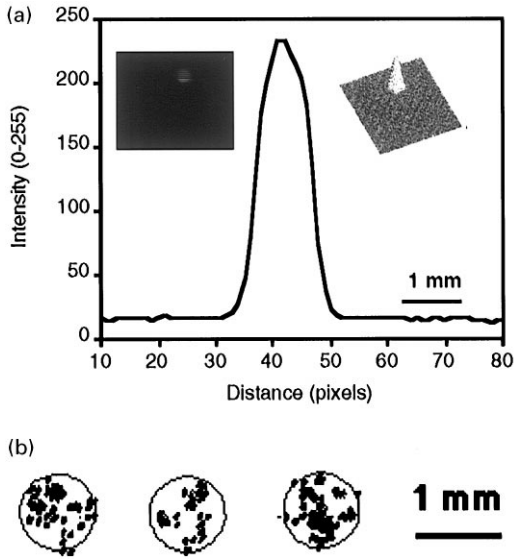

Fig. 7. (a) Insets show the image resulting from the impact of a single ion on the detector, and a wire-frame representation thereof. Main graph is an intensity profile through the center of this image spot. (b) Image showing the location of three 1.0 mm diameter holes (three circles) in a test mask, with the centroids of the light spots from a few 100 ion impacts superposed. The MSP bias was 3.0 kV, and the mesh bias was + 50 V with respect to MSP input. 19.1 keV Ne^{1+} ions were used as the primary irradiation.

of a MSP as the primary detector in a three-dimensional atom probe. For this purpose the detector was operated in a setup similar to an optical atom probe [15]. A typical image spot, obtained with the combination of a Digital Vision Technologies MICAM VHR1000 CCD sensor equipped with a 12.5 mm f 1 : 1.3 lens, and a Scion Corporation LG-3 PCI frame grabber card is shown in Fig. 7a. No image intensification was used between the phosphor screen and the camera, yet the range of light intensities obtained from the detector match the dynamic range of the imaging system. The size of the charge footprint from single detection events was typically 1.0 mm in diameter. The location of the centroids of image spots resulting from impacts of single ions transmitted through a test mask with three 1.0 mm diameter holes held 5 mm in front of the MSP input surface is shown in Fig. 7b. Although the number of ions collected was relatively small, the image suggests from the lack of image spots positioned outside the mask holes that spatial resolution obtained is better than 300 μm FWHM. Other workers have reported positioning errors of 140 μm FWHM [10] and 250 μm FWHM [7]. On a detector with 60 mm diameter effective area, the most conservative of the above values (300 μm FWHM) would result in ~200 pixels across the detector, which would give an effective pixel size of 0.1 nm for a typical area of analysis of 20 nm across, which is sufficient for use in a three-dimensional atom probe application.

A strong non-uniformity in the distribution of the centroids is suggested in Fig. 7b. This appears to be on the same scale as the granularity observed in Fig. 2d and this would lead to some small-scale non-uniformity in the 3DAP images. Note that this non-uniformity does not necessarily reflect variations of detection efficiency across the input surface. This is at least partially due to preferred paths ("channels") for electron multiplication within the MSP, possibly due to the randomness in their architecture, as has been demonstrated by Tremsin et al. [8].

4. Conclusions

The image performance of a MSP is not sufficient for obtaining high-quality field ion images, due to the lack of spatial resolution and granularity observed in the images. However, the imaging performance should be sufficient for aligning, focusing or selecting an area for analysis in (3D) atom probe applications. The spatial resolution obtained from centroiding single ion impacts should be adequate for use in a 3DAP detector.

Gain, pulse height resolution, and temporal resolution obtained from one double thickness MSP are sufficient for use in a time-of-flight single atom sensitivity detector. The detection efficiency was estimated to be ~42%. The operation of the MSP detector was successfully demonstrated in a typical atom probe application.

Acknowledgements

The authors would like to thank Drs. G.W. Fraser (Department of Physics and Astronomy,

University of Leicester, UK) and A.S. Tremsin (Space Sciences Laboratory, University of California, Berkeley, USA) for helpful discussions. Dr. N.D. Evans and K.F. Russell are acknowledged for technical assistance. This research was conducted using the SHaRE Facilities at Oak Ridge National Laboratory (ORNL) and was sponsored by the Division of Materials Sciences, US Department of Energy, under contract DE-AC05-96OR22464 with Lockheed Martin Energy Research Corp. and by an appointment (SJS) to the ORNL Postdoctoral Research Associates Program administered jointly by the Oak Ridge Institute for Science and Education and ORNL.

References

[1] M.K. Miller, G.D.W. Smith, Atom Probe Microanalysis, Principles and Applications to Materials Problems, Materials Research Society, Pittsburgh, PA, 1989.
[2] J.L. Wiza, Nucl. Instr. and Meth. 162 (1979) 587.
[3] T. Sakurai, T. Hashizume, Rev. Sci. Instrum. 57 (1986) 236.
[4] R. Naaman, Z. Vager, Rev. Sci. Instrum. 67 (1996) 3332.
[5] S.J. Sijbrandij, A. Cerezo, B. Deconihout, T.J. Godfrey, G.D.W. Smith, J. Phys. IV (Paris) (Suppl. III) 6 (1996) C5–297.
[6] A.S. Tremsin, J.F. Pearson, J.E. Lees, G.W. Fraser, Proc. SPIE 2578 (1995) 384.
[7] A.S. Tremsin, J.F. Pearson, J.E. Lees, G.W. Fraser, Nucl. Instr. and Meth. A 368 (1996) 719.
[8] A.S. Tremsin, J.F. Pearson, J.E. Lees, G.W. Fraser, V. Korobov, I. Shariv, Nucl. Instr. and Meth. A 392 (1997) 354.
[9] A.S. Tremsin, S.R. Jelinsky, O.H.W. Siegmund, Proc. SPIE 3114 (1997) 272.
[10] J.S. Lapington, L.B.C. Worth, M.W. Throw, Proc. SPIE 2518 (1995) 376.
[11] L.B.C. Worth, J.S. Lapington, M.W. Throw, Nucl. Instr. and Meth. A 392 (1997) 364.
[12] S.J. Sijbrandij, Development and application of an energy compensated three-dimensional atom probe, D. Phil. Thesis, University of Oxford, 1996, pp. 129–130.
[13] M.K. Miller, J. Phys. (Paris) 47 (1986) C7–493.
[14] B. Deconihout, P. Gerard, M. Bouet, A. Bostel, Appl. Surf. Sci. 94/95 (1996) 422.
[15] M.K. Miller, Surf. Sci. 266 (1992) 494.